

Article

Synthesis, Characterization, and Applications of Silver Nano Fibers in Humidity, Ammonia, and Temperature Sensing

Haroon-Ur Rashid ^{1,2,*}, Muhammad Ali ^{1,2}, Mahidur R. Sarker ^{3,*}, Sawal Hamid Md Ali ⁴, Naseem Akhtar ⁵, Nadir Ali Khan ¹, Muhammad Asif ¹ and Sahar Shah ⁶

¹ Department of Electronics, University of Peshawar, Peshawar 25120, Pakistan; ali.muhammad@uop.edu.pk (M.A.); nakhan@uop.edu.pk (N.A.K.); m.asif@uop.edu.pk (M.A.)

² Materials Research Laboratory, Department of Physics, University of Peshawar, Peshawar 25120, Pakistan

³ Institute of IR 4.0, Unversity Kebangsaan Malaysia, Bangi 43600, Malaysia

⁴ Department of Electrical, Electronic and Systems Engineering, Faculty of Engineering and Built Environment, University Kebangsaan Malaysia, Bangi 43600, Malaysia; sawal@ukm.edu.my

⁵ Department of Chemistry, Bacha Khan University Charsadda, Charsadda 24420, Pakistan; nasimakhtarchd@gmail.com

⁶ School of Physics and Electronics, Central South University, Changsha 410083, China; sahar-shah@ele.qau.edu.pk

* Correspondence: haroon.rashid@uop.edu.pk (H.-U.R.); mahidursarker@ukm.edu.my (M.R.S.)

Abstract: The promising chemical, mechanical, and electrical properties of silver from nano scale to bulk level make it useful to be used in a variety of applications in the biomedical and electronic fields. Recently, several methods have been proposed and applied for the small-scale and mass production of silver in the form of nanoparticles, nanowires, and nanofibers. In this research, we have proposed a novel method for the fabrication of silver nano fibers (AgNFs) that is environmentally friendly and can be easily deployed for large-scale production. Moreover, the proposed technique is easy for device fabrication in different applications. To validate the properties, the synthesized silver nanofibers have been examined through Fourier transform infrared spectroscopy (FTIR), scanning electron microscopy (SEM), and X-ray diffraction (XRD). Further, the synthesized silver nanofibers have been deposited over sensors for Relative humidity (RH), Ammonia (NH₃), and temperature sensing applications. The sensor was of a resistive type, and found 4.3 kΩ for relative humidity (RH %) 30–90%, 400 kΩ for NH₃ (40,000 ppm), and 5 MΩ for temperature sensing (69 °C). The durability and speed of the sensor verified through repetitive, response, and recovery tests of the sensor in a humidity and gas chamber. It was observed that the sensor took 13 s to respond, 27 s to measure the maximum value, and took 33 s to regain its minimum value. Furthermore, it was observed that at lower frequencies and higher concentration of NH₃, the response of the device was excellent. Furthermore, the device has linear and repetitive responses, is cost-effective, and is easy to fabricate.

Keywords: silver nanoparticles; nanofibers; humidity; ammonia; temperature sensor



Citation: Rashid, H.-U.; Ali, M.; Sarker, M.R.; Md Ali, S.H.; Akhtar, N.; Khan, N.A.; Asif, M.; Shah, S. Synthesis, Characterization, and Applications of Silver Nano Fibers in Humidity, Ammonia, and Temperature Sensing. *Micromachines* **2021**, *12*, 682. <https://doi.org/10.3390/mi12060682>

Received: 3 May 2021

Accepted: 31 May 2021

Published: 10 June 2021

Publisher's Note: MDPI stays neutral with regard to jurisdictional claims in published maps and institutional affiliations.



Copyright: © 2021 by the authors. Licensee MDPI, Basel, Switzerland. This article is an open access article distributed under the terms and conditions of the Creative Commons Attribution (CC BY) license (<https://creativecommons.org/licenses/by/4.0/>).

1. Introduction

Nowadays, nanoparticles (NPs) are gaining great interest because of their nanostructure, small size, large surface area, high thermal stability, and excellent physical and chemical properties, which cannot be achieved by bulk materials [1]. A small size (ranging from 1 nm to 100 nm) [2], one dimension [3], and a large surface area allow these NPs to attach to biological entities without changing their properties and function. Some materials behave differently at the nanoscale, and they emerge with new characteristics, like aluminum, as they become explosive or their melting point changes. Similarly, AgNPs have revealed new properties and act as antibacterial agents [4]. However, recent studies on NPs and nanofibers showcase the potential risks of NP aerosol release, and allow amore balanced benefit/risk analysis. For example, many studies highlight NP emissions due to

coatings, paints [5], and tiles [6]. Cases of NPs exposure in the field of occupational hygiene at coating workplaces have been reported [7]. A small size and a large surface area permit NPs to make strong bonds with surfactant molecules. Among these physical and chemical applications of NPs, silver nanoparticles (AgNPs) have become the main focusing area for the researchers in the field of nanotechnology [8]. AgNPs can be used in anti-bacterial agents, medical applications, food, and healthcare. AgNPs can also be used in anti-bacterial coatings, wound dressings found in socks, refrigerators, and sports clothing because they have the ability to kill germs [9]. AgNPs can also be used in liquid form for coatings and sprays within a shampoo [10]. Similarly, AgNPs in the form of silver nanofibers (AgNFs) can be employed in water purification systems as a filtration membrane [11] that stores silver ions, forming a thin membrane layer that creates a protective barrier against bacteria and fungi. Also, the small size and large surface area [12–15] of AgNFs enhances their detection and response capability.

In this article, uniform silver nanofibers (AgNFs) are formed through a simple and cost-effective technique called electrospinning [16] with a controlled diameter [17] of nano-size in the fabrication of a sensor for sensing relative humidity, gas, and temperature with rapid response and recovery time because the relative humidity is not only important for human comfort but also important for different industries and technologies [18]. A practical humidity sensor must have the properties of excellent sensitivity, quick response and recovery time, chemical and thermal stability, and repeatability. Humidity sensors are of two types reported so far, one is the capacitive type [19] and the other is a resistive type [20]. A capacitive typesensor is used for polymers. A capacitive humidity sensor is noticed against the water molecules present in the air. The second type of humidity sensor is a resistive type whose resistance changes with water molecules. A resistive type humidity sensor is used for conductive materials like metals, copper, and silver. Similarly, permanent monitoring is needed for our surrounding environment to prevent the proliferation of toxic gases [21] such as NH_3 , which is a colorless and poisonous gas present in our atmosphere that has a great impact on various fields such as the industrial, chemical, and medical fields. NH_3 at a higher concentration in the atmosphere can affect the human body and cause irritation of the eyes, throat infections, skin infections, and respiratory problems. For this reason, many sensors have been used so far like metal oxide gas sensors [22], catalytic ammonia detectors [23,24], optical ammonia [25], conductive polymer sensors [26,27], solid-state gas sensors [28], polyamine base ammonia detection, optical gas analyzers, and reduced graphene oxide thin films, but quick response and recovery is the main problem associated with these sensors [29–31]. Also, the temperature is the main factor affecting the lifestyles of living things. It is the degree of hotness or coldness of a place measured in Kelvin, Fahrenheit, and Celsius. Temperature plays an important role in many fields, which is important for the mechanism that is used in medical drugs, liquids, laboratories, cosmetics products, goods, ICs fabrications, aerospace and defense, automotive, and many other fields. The accuracy of the temperature during the manufacturing is very important for quality control.

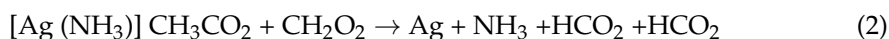
Herein, we report the synthesis of AgNPs through a chemical method, fabrication of AgNFs by an electrospinning technique, and its sensing applications in relative humidity, gas and temperature sensing. It seems from the results that AgNFs exhibits superior sensing properties towards RH, NH_3 , and Temperature.

2. Experimental Work

2.1. Synthesis of Silver Nano Particles (AgNPs)

Before the synthesis of AgNFs, it is necessary to synthesize AgNPs [32]. For this purpose, a chemical method was used by taking 1 gm of silver acetate (AgCH_3O_2) and 2.5 mL of NH_3 bought from Sigma Aldrich ChemieGmbH. Add the NH_3 dropwise to the silver acetate and stir for a few minutes at 40 °C until the solution is completely dissolved (black color). Then add drop wise 0.2 mL formic acid (CH_2O_2) to the solution, and an exothermic reaction will take place according to the chemical formula and the solution

turns into a grey color. Keep the solution for a night to settle down the particles at the bottom. The solution is then filtered through a 0.2 μm syringe filter. Finally, a transparent solution [33] is obtained called AgNPs.



2.2. Fabrication of Silver Nano Fibers (AgNFs)

For the synthesis of AgNFs, polyvinyl alcohol (PVA) solution (2 gm PVA and 20 mL distilled water) was added to 2 mL AgNPs, which was 10% of the total weight of the solution. The solution was stirred at 140 °C at 350 r.p.m. Its viscosity was checked because at lower concentration electro spray occurs instead of electrospinning which creates a mixture of fibers and beads [34]. For the synthesis of AgNFs through the electrospinning technique, the AgNPs solution was loaded in a medical/plastic syringe. The positive terminal of the power supply connected with the tip of the needle of the plastic syringe containing the solution. The negative terminal of the power supply was connected to the electrospinning collector. Aluminum foil was wrapped around the collector side. A power supply of 15 kva was used in the electrospinning unit. The distance between the tip of the needle and collector was kept from 12 cm to 16 cm. A 12 v.d.c motor was used in the electrospinning unit to push forward the plastic syringe for the continuous flow of solution. Also, the speed of the motor was kept at a minimum speed to prevent the solution from spoiling. Composite and uniform AgNFs were fabricated at the collector side [35].

3. Characterizations

Before the material can be used in different applications, it is necessary to characterize the physical and chemical properties, size, structure, and diameter of the AgNFs. For this purpose, different analytical techniques were used including Fourier transform infrared spectroscopy (FTIR), scanning electron microscopy (SEM), and X-ray diffraction (XRD). After analyzing, the AgNFs were then used for relative humidity, temperature and ammonia sensing. The flow chart for the whole research methodology used is shown in Figure 1.

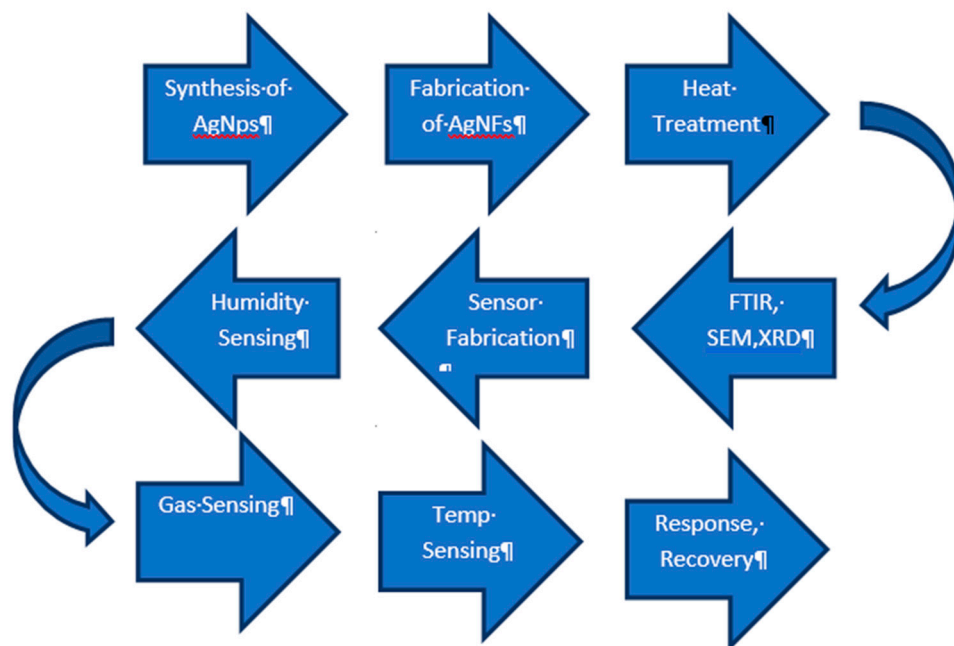


Figure 1. Flow chart for the research methodology, characterization, fabrication, and sensing.

3.1. Fourier Transform Infrared Spectroscopy (FTIR)

The FTIR of AgNPs was performed to check the bond formation using Perkin Elmer FTIR spectrometer machine model spectrum two, serial number 103385, scan speed 0.2, IR-Laser Wave number 11,750.00, Wavelength ranging from 4000 cm^{-1} to 450 cm^{-1} , as shown in Figure 2.

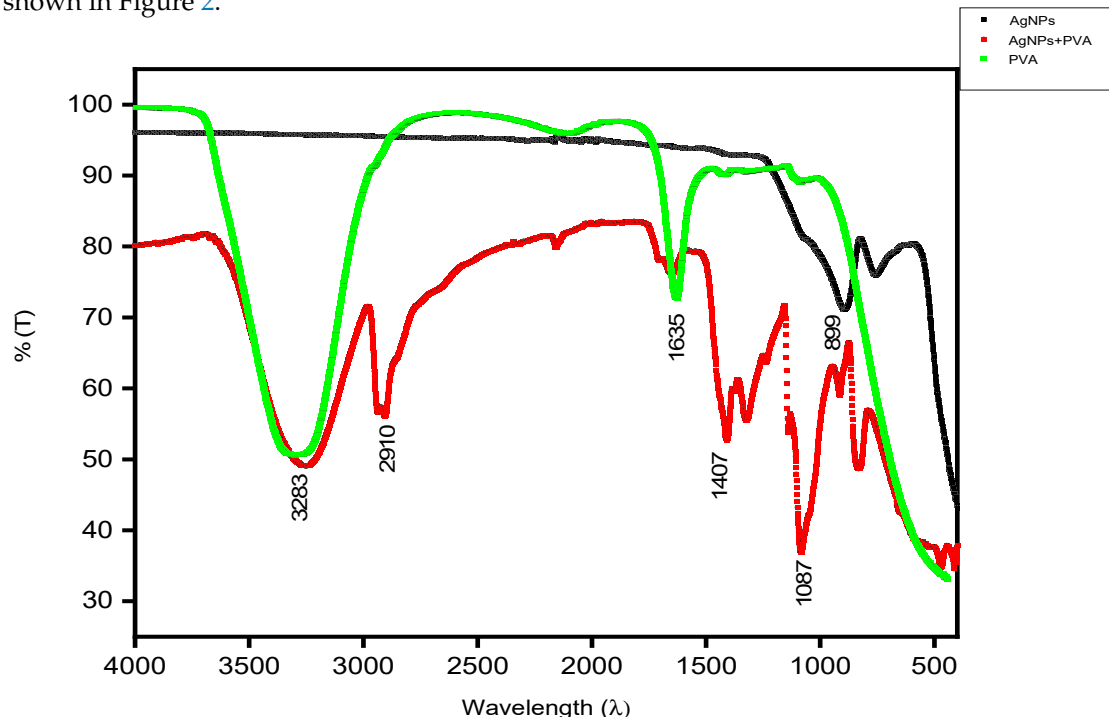


Figure 2. FTIR of AgNPs + PVA (red), PVA (green), and AgNPs (black).

The FTIR of AgNPs (black curve) shows an absorption peak at 899 cm^{-1} , representing O-H aromatic compounds. After adding PVA solution to the AgNPs for the fabrication of silver nanofibers, the final FTIR was conducted (red curve). The peaks show the bond formation at 3283 cm^{-1} corresponding to O-H vibration, 2910 cm^{-1} shows C-H stretching, 1407 cm^{-1} shows C-H₂ methylene groups, 1087 cm^{-1} shows C=O stretching, which shows a strong bond between 80%T to 40%T. Moreover, FTIR of PVA (green) in pure form was done and the peaks reported at wavelengths 3283 cm^{-1} and 1635 cm^{-1} .

3.2. Scanning Electron Microscopy (SEM)

The structure and diameter of the AgNFs investigated through scanning electron microscopy (SEM), serial numbered JEOL 5910 SEM with a magnification range of 10X–300 K X and tungsten electronic beam energies in the range 1–40 keV. The diameter of the fibers was calculated through image J software. The fiber diameter investigated was uniform. As shown in Figure 3a, the diameters of nanofibers were 166 nm, Figure 3b 333 nm, Figure 3c 208 nm, and Figure 3d 285 nm.

3.3. X-ray Diffraction (XRD)

Using a PANalytical-X'Pert³ powder X-ray diffractometer equipped with CuK α 1 radiation ($=1.54056\text{ \AA}$), installed in the materials research laboratory (MRL), Department of Physics, University of Peshawar, the XRD of AgNFs calcined at $350\text{ }^\circ\text{C}$ was performed. The X-ray diffraction patterns were recorded at 2θ ranging from 10° to 70° with a scan speed of $1^\circ/\text{min}$ and step size of 0.020. Furthermore, the values set for voltage and current during the operation were 45 kV and 40 mA, respectively. A single phase of silver was reported, which confirmed the single composite nanofibers with no additional phases. The structure and peaks of the silver were matched using MATCH software. It was confirmed that

the fiber structure was cubic. Peaks were found at angles 38° , 44° , and 64° , as shown in Figure 4.

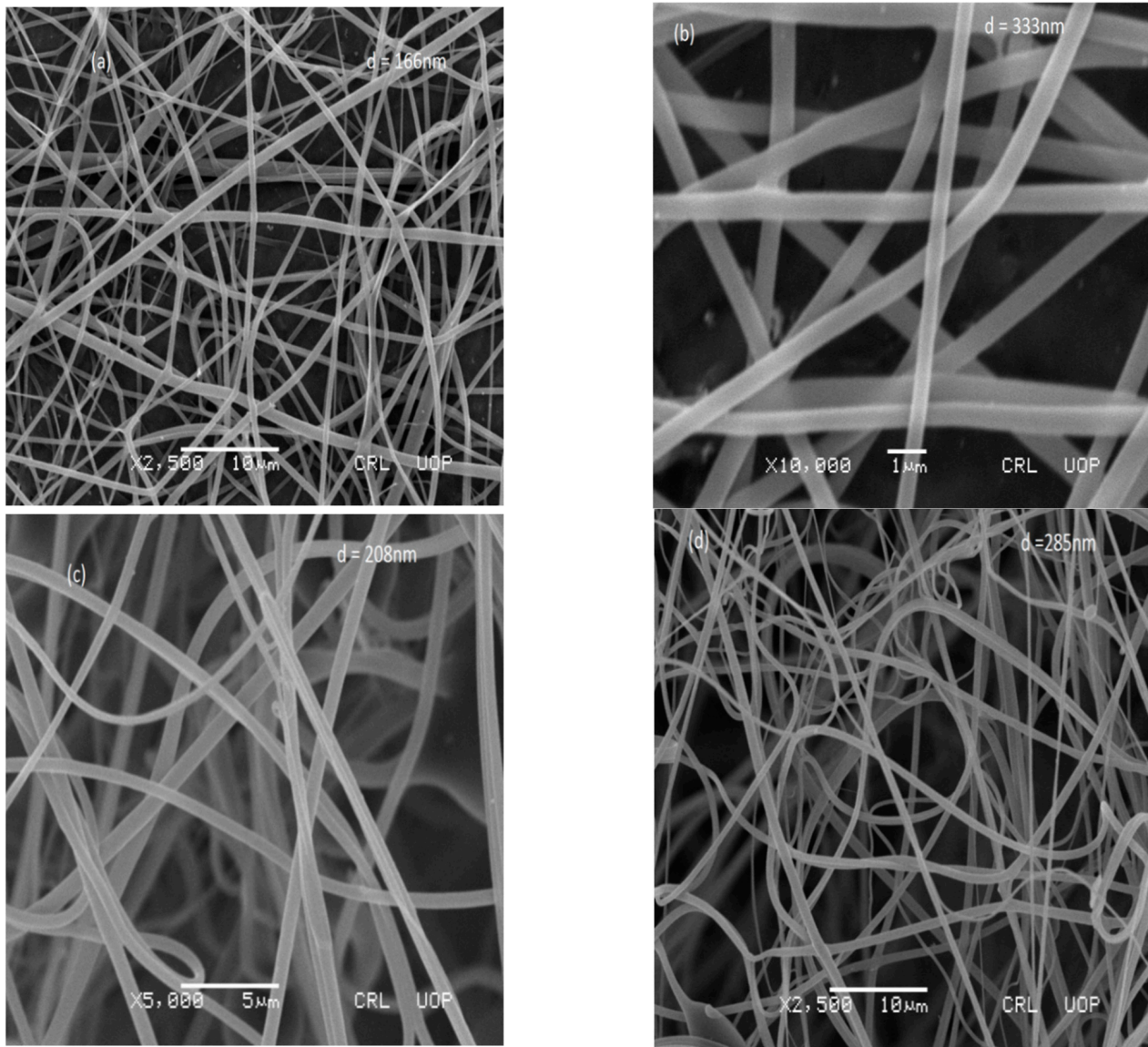


Figure 3. (a–d): SEM images with diameters in nanometers.

3.4. Fabrication of Sensor

The interdigitated electrodes (IDE) used in many applications [36–38] were fabricated by depositing the AgNFs layer by electrospinning over it. After the deposition of AgNFs, the device was dried in an oven at 100°C for 1 h. The distance between the comb fingers and the width of the comb fingers is 0.21 mm. The length, width, and thickness of the substrate are 14, 7, and 1 mm respectively (0.5 mm Alumina & 0.5 mm Copper layer). The schematic is given below. The entire process of sensor fabrication and schematic of the device is given in Figure 5a,b.

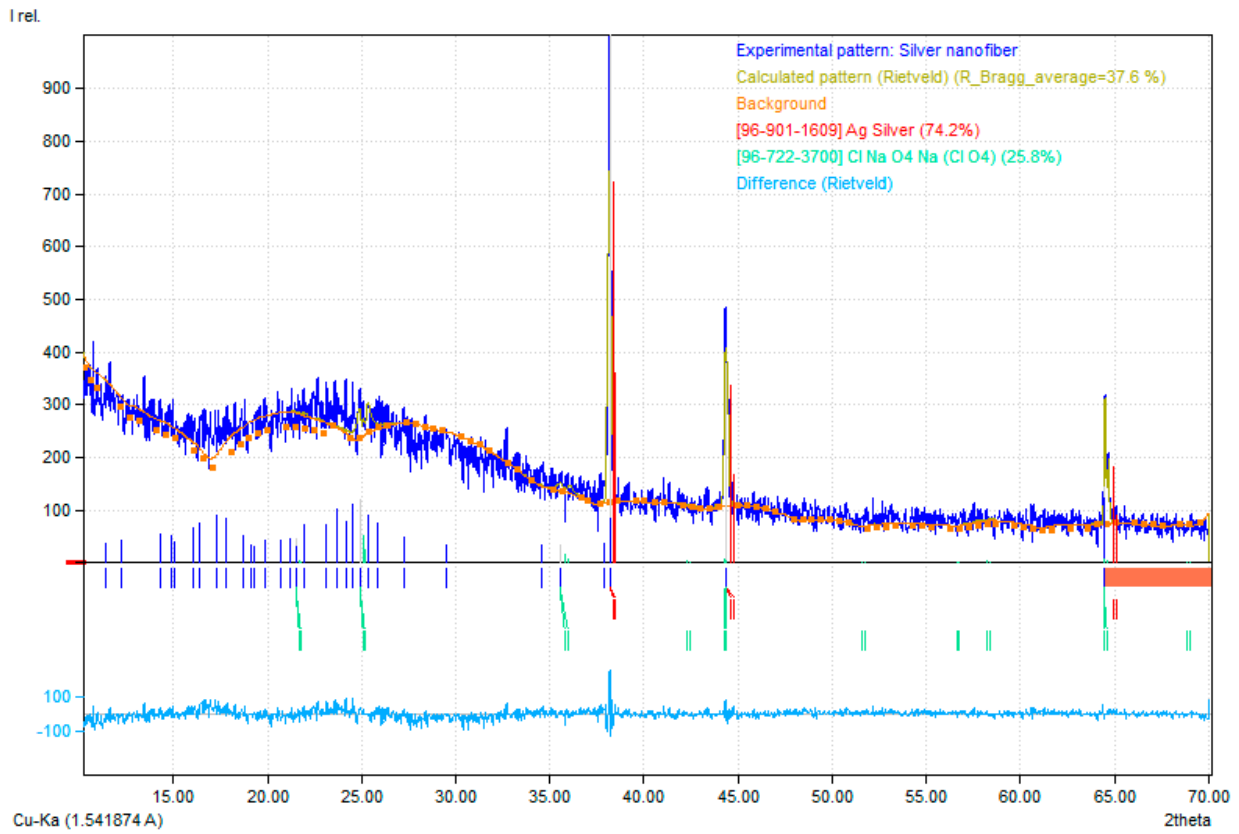


Figure 4. X-ray Diffractionspectrumof Silver nanofibers.

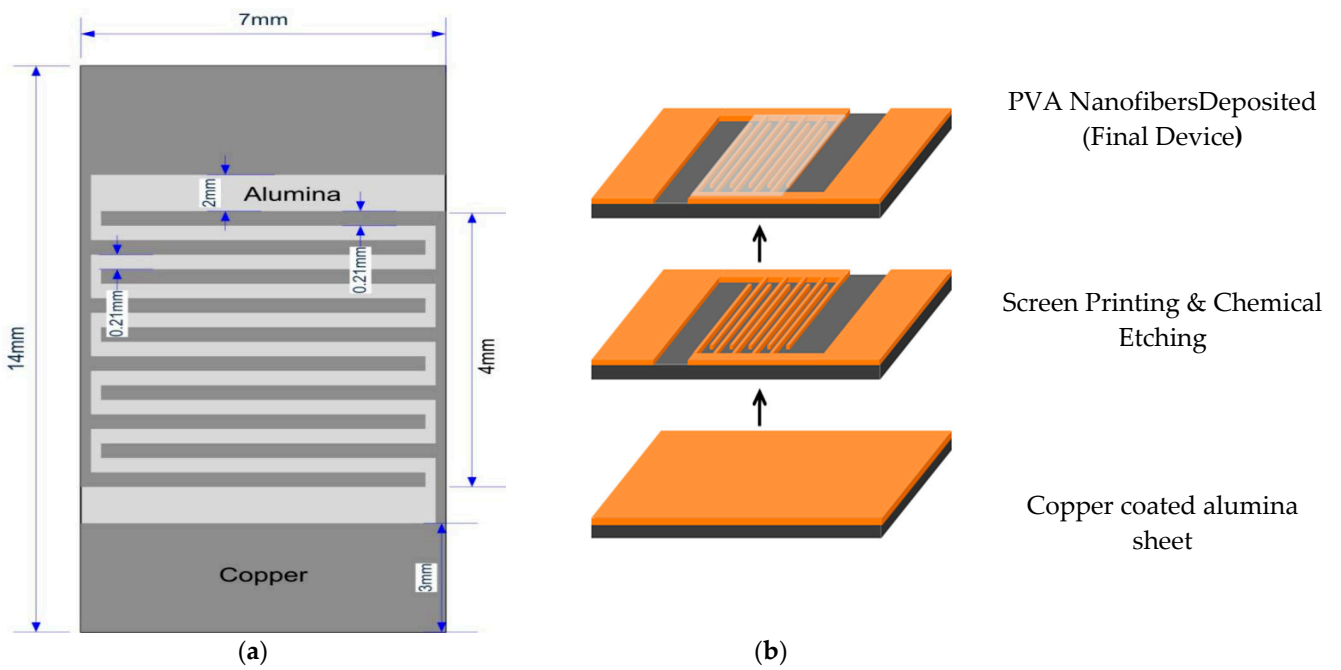


Figure 5. (a) Dimention (b) Printed diagram of interdigitated electrode.

4. Results and Discussion

4.1. Relative Humidity

The AgNFs deposited IDE was kept in a humidity chamber and resistance vs. RH (%) was investigated. Inside the chamber, the resistance of the IDE was calculated with respect to time and water molecules. It was observed that the resistance of IDE increases linearly with RH (%) [39], as shown in Figure 6.

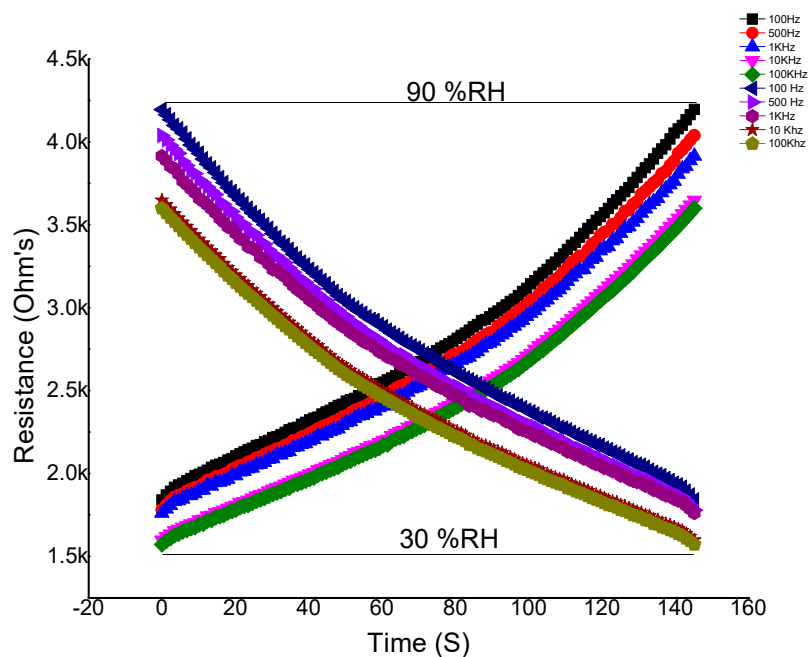


Figure 6. Relative humidity (30–90%), frequency, and time vs. resistance.

The resistive response of the sensor was investigated at different frequencies, i.e., 100 Hz, 500 Hz, 1 kHz, 10 kHz, 100 kHz, and 1 MHz. It was observed that the response of the sensor is not very good at higher frequencies. The sensor shows excellent behavior up to 10 kHz. As the graph shows, relative humidity was measured from 30–90%RH, and the resistance was 4.3 k Ω from 100 Hz to 10 kHz.

It is clear from the graph that measuring relative humidity from 30% to 90%, the sensor took 145 s to respond to maximum relative humidity and the resistance was 4.3 k Ω in the forward direction (curves starting from 0 s). The same experiment was repeated in the reverse direction (curves from 4.3 k Ω to 160 s), and the same data was investigated. Both the curves were found to be the same, which means that the sensor shows excellent response and recovery in both directions over equal intervals of time. It proved that the sensor is linear and has good performance.

4.2. Ammonia Sensing

The sensing device is also used to sense toxic gasses like NH₃. The sensor shows a good response to NH₃. For this purpose, different frequencies ranging from 100 Hz to 1 MHz were used. A resistance vs ammonia concentration (ppm) graph was noted. It was found that at 100 Hz and 1 kHz, the resistance was 400 k Ω , and NH₃ molecules were 40,000 ppm, which means that the sensor is a resistive type and shows excellent behavior towards NH₃ molecules as shown in Figure 7.

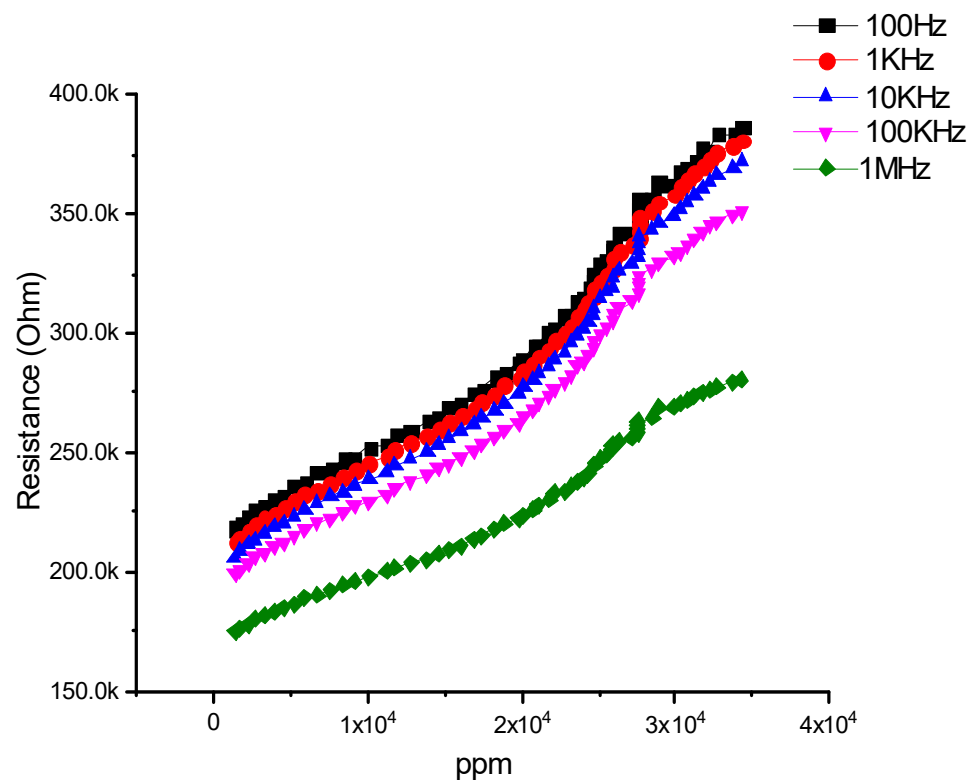


Figure 7. Resistance (ohm) vs. concentration of ammonia (ppm).

It was also noted that the resistance is directly proportional to ppm. Resistance and ppm were co-linear. Resistance increases as ppm increases [40]. It was also confirmed that at low frequencies the response of the sensor is excellent compared to higher frequencies.

4.3. Silver Nanofibers Sensor vs. Temperature

It is obvious that most conducting materials change their resistance with temperature [41]. That is why specific resistance of a specific material is specified with standard temperatures. IDE coated with AgNFs was used as a temperature sensor by calculating its temperature with respect to resistance. The main idea is to confirm that the sensor is not affected by temperatures up to 69 °C. The resistance increases with temperature that mean that the sensor has a positive temperature coefficient [42]. It was observed that at 5 MΩ, the temperature was 69 °C, as shown in Figure 8.

4.4. Response and Recovery Time

For an excellent sensing device, it is important that it exhibits a rapid response and recovers to its initial state in a short period of time. To check the performance of the designed sensing device, response and recovery measurements of the device have been performed, as shown in Figure 9. From the figure, it was observed that the device shows a maximum resistive sensitivity at lower frequencies due to skin or surface effect, because the gas molecules directly interact with the surface of the material and at lower frequency skin effect is dominant over a bulk material. Also, the device sensitivity was observed at different concentrations of NH₃ in parts per million (ppm). When the device is exposed to NH₃ in a chamber, the gas molecules interact with the surface of the sensing material and thus increase the resistance of the device from 25 kΩ to 450 kΩ at 100 Hz and 1 kHz, respectively. The response time is the time from the initial state to the maximum saturation state of the device, while the recovery time is the period from maximum saturation back to the initial state. The maximum response time of the device observed was 27 s (from 49 to 71 s on the x-axis time scale) at 20,000 ppm (blue strip) while the maximum recovery time of the device was observed at 33 s at 10,000, ppm highlighted in yellow in Figure 9.

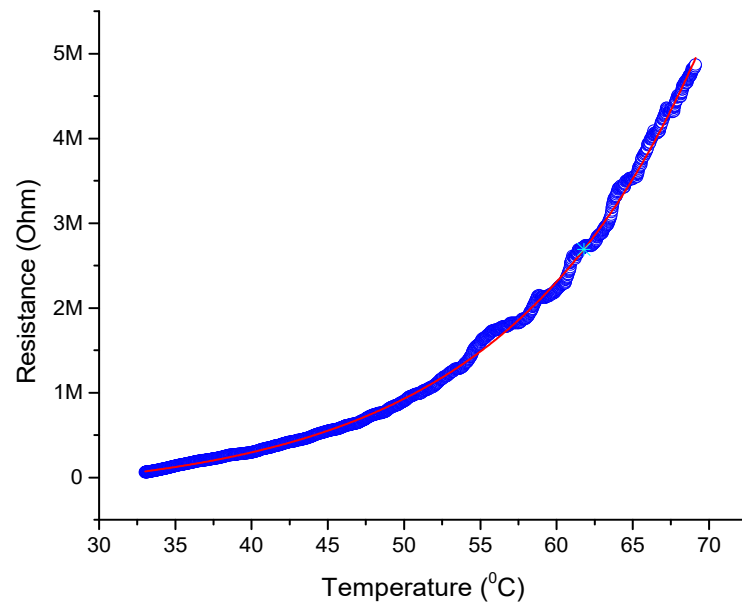


Figure 8. Resistance of the fabricated silver nanofibers sensor vs. temperature.

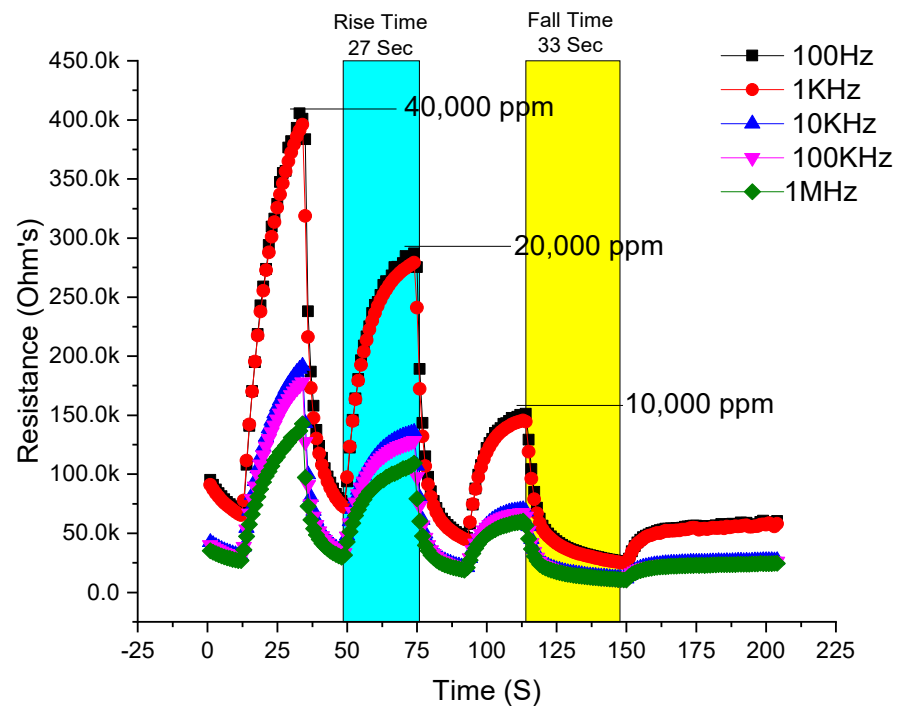


Figure 9. Response (rise of the curve) and recovery (fall of the curve) of the ammonia sensor.

5. Conclusions

In this research, the structural morphology, chemical, and physical properties of silver nanofibers (AgNFs) have been studied. Different techniques have been performed for characterization, and the results led to the following conclusions.

AgNPs have been synthesized using ammonia, formic acid, and silver acetate through a chemical method. The AgNPs obtained were transparent in color. The AgNPs solution (2 mL) was then added to 20 mL of PVA solution to synthesize AgNFs through the electro-spinning technique. The synthesized AgNFs were then kept in the oven to dry at 90 °C. The dried fibers were then kept in the furnace at 350 °C for 2 h to calcine and to reduce the diameter of the fibers.

SEM images show the diameter of the nanofibers in nanometers. The FTIR of nanofibers shows the chemical bond formation at wavelengths, 3283 cm^{-1} , 2910 cm^{-1} , 1635 cm^{-1} , 1407 cm^{-1} , 1087 cm^{-1} , and 899 cm^{-1} . The calcined nanofibers were then characterized through XRD. Peaks reported at 38° , 44° , and at 64° with intensities of 740, 200, and 170, respectively. The AgNFs were found to be cubic in shape.

The AgNFs deposited IDE device was used for sensing relative humidity, and it was found to be of a resistive type. At $4.3\text{ k}\Omega$, the relative humidity was 90%. The response and recovery time of the sensor was noted, which was 145 s. It was reported that at lower frequencies the device shows excellent behavior i.e., at 100 Hz and 10 kHz, the relative humidity was 90%.

The sensor was then used for temperature sensing and it was found that the sensor has a positive temperature coefficient. It was observed that at $0.5\text{ M}\Omega$ the temperature was 45°C , at $1.5\text{ M}\Omega$ the temperature was 55°C , and at $5\text{ M}\Omega$ the temperature was 69°C , which means that resistance increases with temperature.

Similarly, the sensor was used for gas sensing applications for ammonia. It was found that at 100 Hz and 1 kHz, the resistances measured were $400\text{ k}\Omega$, $275\text{ k}\Omega$, and $150\text{ k}\Omega$ for NH_3 concentrations of 40,000 ppm, 20,000 ppm, and 10,000 ppm, respectively. The sensor starts sensing after 13 s, and takes 27 s (rise time) to respond to ammonia molecules to their maximum value and after releasing ammonia molecules it returns to its original value after 33 s (fall time), which shows slow recovery at a lower concentration of ammonia.

Finally: it was concluded that the device has a linear and repetitive response, is cost-effective, and is easy to fabricate. Also, it seems from the results that AgNFs exhibits superior sensing properties towards RH, NH_3 , and temperature.

Author Contributions: The authors contributed to this manuscript in the given terms H.-U.R. Experimental work, data compilation, Methodology, data analysis, paper writing. M.A. (Muhammad Ali) Co-supervisor, ideas, software programming, data analyst. M.R.S. Corresponding author, investigation. S.H.M.A. project advisor, analyst, formal analysis. N.A. Environmental analyst, software, review and editing. N.A.K. Supervisor, Resources. M.A. (Muhammad Asif) Formal analysis wireless communication. S.S. Wireless communication, sensor response and recovery analyst. All authors have read and agreed to the published version of the manuscript.

Funding: The authors acknowledge the financial support of university Kebangsaan Malaysia under the Grant Code GPK-C19-2020-013.

Institutional Review Board Statement: Not applicable.

Informed Consent Statement: Not applicable.

Data Availability Statement: Not applicable.

Conflicts of Interest: The authors declare no conflict of interest.

References

1. United Nations. Questions about Nanotechnology. 2012. Available online: <https://www.epa.gov/chemical-research/research-nanomaterials> (accessed on 21 September 2020).
2. Jeevanandam, J.; Barhoum, A.; Chan, Y.S.; Dufresne, A.; Danquah, M.K. Review on nanoparticles and nanostructured materials: History, sources, toxicity and regulations. *Beilstein J. Nanotechnol.* **2018**, *9*, 1050–1074. [[CrossRef](#)] [[PubMed](#)]
3. Kumar, N.; Kumbhat, S. *Essentials in NanoScience and Nanotechnology*; Wiley: Hoboken, NJ, USA, 2016.
4. Norsuzila Ya'acob, Mardina Abdullah and Mahamod Ismail et al. *Intech* **1989**, *32*, 137–144.
5. Morgenev, M.; Aguerre-Chariol, O.; Bressot, C. STEM imaging to characterize nanoparticle emissions and help to design nanosafe paints. *Chem. Eng. Res. Des.* **2018**, *136*, 663–674. [[CrossRef](#)]
6. Bressot, C.; Aubry, A.; Pagnoux, C.; Aguerre-Chariol, O.; Morgenev, M. Assessment of functional nanomaterials in medical applications can time mend public and occupational health risks related to the products' fate? *J. Toxicol. Environ. Health* **2018**, *81*, 957–973. [[CrossRef](#)] [[PubMed](#)]
7. Bressot, C.; Shandilya, N.; Jayabalan, T.; Fayet, G.; Voetz, M.; Meunier, L.; Le Bihan, O.; Aguerre-Chariol, O.; Morgenev, M. Exposure assessment of Nanomaterials at production sites by a Short Time Sampling (STS) approach Strategy and first results of measurement campaigns. *Process. Saf. Environ. Prot.* **2018**, *116*, 324–332. [[CrossRef](#)]

8. Rosli, M.M.; Aziz, T.H.T.A.; Zain, A.R.M.; Alias, N.; AbdMalek, N.A.; Abdullah, N.A.; Saad, S.K.M.; Umar, A.A. Micro-strain effect on electronic properties in graphene induced by silver nanowires. *Physica E* **2020**, *123*, 114203. [[CrossRef](#)]
9. Nakamura, P.; Shingo, W.; Masahiro, S.; Yoko, S.; Naoko, A.; Tomohiro, Y.; Takayama, M.; Masanori, F.; Masayuki, I. Synthesis and application of silver nanoparticles (Ag NPs) for the prevention of infection in healthcare workers. *Int. J. Mol. Sci.* **2019**, *20*, 3620. [[CrossRef](#)]
10. Lovell, A. Inventory finds increase in consumer products containing nanoscale materials. In *Relaunched Inventory Seeks Input to Address Scientific Uncertainty*; Wilson Centre: Washington, DC, USA, 2013; Volume 28.
11. Fang, J.; Wang, X.; Lin, T.; Lin, T. (Eds.) *Nanofibers: Production, Properties and Functional Applications*; Intech: London, UK, 2011; ISBN 9789533074207.
12. Huang, X.J.; Choi, Y.K. Chemical sensors based on nanostructured materials. *Sens. Actuators B* **2007**, *122*, 659–671. [[CrossRef](#)]
13. Zhao, H.; Chen, Y.; Quan, X.; Ruan, X. Preparation of Zn-doped TiO₂ nanotubes electrode and its application in pentachlorophenol photoelectrocatalytic degradation. *Chin. Sci. Bull.* **2007**, *52*, 1456–1457. [[CrossRef](#)]
14. Ji, H.; Lu, H.; Ma, D.; Yu, J.; Ma, S. Preparation and hydrogen gas sensitive characteristics of highly ordered titania nanotube arrays. *Chin. Sci. Bull.* **2008**, *53*, 1352–1357. [[CrossRef](#)]
15. Wan, Q.; Li, Q.H.; Chen, Y.J.; Wang, T.H.; He, X.L.; Li, J.P.; Lin, C.L. Fabrication and ethanol sensing characteristics of ZnO nanowire gas sensors. *Appl. Phys. Lett.* **2004**, *84*, 3654–3656. [[CrossRef](#)]
16. Bhardwaj, N.; Kundu, S.C. Electrospinning. *Biotechnol. Adv.* **2010**, *28*, 325–347. [[CrossRef](#)] [[PubMed](#)]
17. Liu, Y.; He, J.H.; Yu, J.Y.; Zeng, H.M. Controlling numbers and sizes of beads in electrospun nanofibers. *Polym. Int.* **2008**, *57*, 632–636. [[CrossRef](#)]
18. Chen, Z.; Lu, C. Humidity sensors: A review of materials and mechanisms. *Sens. Lett.* **2005**, *3*, 274–295. [[CrossRef](#)]
19. Kim, J.H.; Hong, S.M.; Moon, B.M.; Kim, K. High-performance capacitive humidity sensor with novel electrode and polyimide layer based on MEMS technology. *Microsyst. Technol.* **2010**, *16*, 2017–2021. [[CrossRef](#)]
20. Li, L.; Vilela, F.; Forgie, J.; Skabara, P.J. Miniature humidity micro-sensor based on organic conductive polymer-poly (3, 4-ethylenedioxythiophene). *Micro Nano Lett.* **2009**, *4*, 84–87. [[CrossRef](#)]
21. Qi, Q.; Zhang, T.; Liu, L.; Zheng, X.; Lu, G. Improved NH₃, C₂H₅OH, and CH₃COCH₃ sensing properties of SnO₂ nanofibers by adding block copolymer P123. *Sens. Actuators B* **2009**, *141*, 174–178. [[CrossRef](#)]
22. Zakrzewska, K. Mixed oxides as gas sensors. *Thin Solid Film.* **2001**, *391*, 229–238. [[CrossRef](#)]
23. Lundström, I.; Svensson, C.; Spetz, A.; Sundgren, H.; Winqvist, F. From hydrogen sensors to olfactory images—Twenty years with catalytic field-effect devices. *Sens. Actuators B* **1993**, *13*, 16–23. [[CrossRef](#)]
24. Naar, S.; Hasan, M.R.; Kadhum, A.A.H.; Hasan, H.A.; Zain, M.F.M. Photocatalytic degradation of organic pollutants over visible light active plasmonic Ag nanoparticle loaded Ag₂SO₃ photocatalysts. *J. Photochem. Photobiol. Chem.* **2019**, *375*, 191–200. [[CrossRef](#)]
25. Strike, D.J.; Meijerink, M.G.H.; Koudelka-Hep, M. Electronic noses—A mini-review. *Fresn. J. Anal. Chem.* **1999**, *364*, 499–505. [[CrossRef](#)]
26. Nicolas-Debarnot, D.; Poncin-Epaillard, F. Polyaniline as a new sensitive layer for gas sensors. *Anal. Chim. Acta* **2003**, *475*, 1–15. [[CrossRef](#)]
27. Alahya, S.N.A.; Hanifah, S.A.; Rozi, N.; AbdKarim, N.H.; Heng, L.Y. Effects of Silver Nanowire-Based Polymer Composite Membrane on The Physical and Electrochemical Properties of Malachite Green Sensor. *Malays. J. Anal. Sci.* **2019**, *23*, 325–335.
28. Dubbe, A. Fundamentals of solid state ionic micro gas sensors. *Sens. Actuators B Chem.* **2003**, *88*, 138–148. [[CrossRef](#)]
29. Olbrechts, B.; Rue, B.; Suski, J.; Flandre, D.; Raskin, J.P. Characterization of FD SOI devices and VCO's on thin dielectric membranes under pressure. *Solid-State Electron.* **2007**, *51*, 1229–1237. [[CrossRef](#)]
30. Wang, D.; Chu, X.; Gong, M. Hydrothermal growth of ZnO nanoscrewdrivers and their gas sensing properties. *Nanotechnology* **2007**, *18*, 185601. [[CrossRef](#)]
31. Franke, M.E.; Koplín, T.J.; Simon, U. Metal and metal oxide nanoparticles in chemiresistors: Does the nanoscale matter? *Small* **2006**, *2*, 36–50. [[CrossRef](#)] [[PubMed](#)]
32. Jamil, A.; Lim, H.N.; Yusof, N.A.; Tajudin, A.A.; Huang, N.M.; Pandikumar, A.; Golsheikh, A.M.; Lee, Y.H.; Andou, Y. Preparation and characterization of silver nanoparticles-reduced graphene oxide on ITO for immune sensing platform. *Sens. Actuators B Chem.* **2015**, *221*, 1423–1432. [[CrossRef](#)]
33. Lau, K.S.; Chin, S.X.; Tan, S.T.; Lim, F.S.; Chang, W.S.; Yap, C.C.; Jumali, M.H.H.; Zakaria, S.; Chook, S.W.; Chia, C.H. Silver nanowires as flexible transparent electrode: Role of PVP chain length. *J. Alloy. Compd.* **2019**, *803*, 165–171.
34. Perez, M.; Ronda, J.C.; Reina, J.A.; Serra, A. Synthesis of functional polymers by chemical modification of PECH and PECH-PEO with substituted phenolates. *Polymer* **2001**, *42*, 261–272.
35. Ji, W.; Sun, Y.; Yang, F.; van den Beucken, J.J.; Fan, M.; Chen, Z.; Jansen, J.A. Bioactive electrospun scaffolds delivering growth factors and genes for tissue engineering applications. *Pharm. Res.* **2011**, *28*, 1259–1272. [[CrossRef](#)]
36. Rauwel, P.; Rauwel, E.; Ferdov, S.; Singh, M.P. Silver nanoparticles: Synthesis, properties, and applications. *Sens. Actuators B Chem.* **1998**, *B49*, 73–80. [[CrossRef](#)]
37. Aoki, K.; Morita, M.; Niwa, O.; Tabei, H. Quantitative analysis of reversible diffusion-controlled currents of redox soluble species at interdigitated array electrodes under steady-state conditions. *J. Electroanal. Chem.* **1988**, *256*, 269–282. [[CrossRef](#)]

38. Lee, C.Y.; Chiang, C.M.; Wang, Y.H.; Ma, R.H. A self-heating gas sensor with integrated NiO thin-film for formaldehyde detection. *Sens. Actuators B Chem.* **2007**, *122*, 503–510. [[CrossRef](#)]
39. Liu, L.; Ye, X.; Wu, K.; Han, R.; Zhou, Z.; Cui, T. Humidity sensitivity of multi-walled carbon nanotube networks deposited by dielectrophoresis. *Sensors (Basel, Switzerland)* **2009**, *9*, 1714–1721. [[CrossRef](#)] [[PubMed](#)]
40. Chen, M.; Wang, W.; Feng, Y.; Zhu, X.; Zhou, H.; Tan, Z.; Li, X. Impact resistance of different factors on ammonia removal by heterotrophic nitrification–aerobic denitrification bacterium *Aeromonas* sp. HN-02. *Bioresour. Technol.* **2014**, *167*, 456–461. [[CrossRef](#)]
41. MacFadden, D.; McGough, S.; Fisman, D.; Santillana, M.; Brownstein, J. Antibiotic resistance increases with local temperature. *Open Forum Infect. Dis.* **2017**, *4*, S179. [[CrossRef](#)]
42. Zeng, Y.; Lu, G.; Wang, H.; Du, J.; Ying, Z.; Liu, C. Positive temperature coefficient thermistors based on carbon nanotube/polymer composites. *Sci. Rep.* **2014**, *4*, 6684. [[CrossRef](#)] [[PubMed](#)]